

Oxygen-sensing properties of ormosil hybrid materials doped with ruthenium(II) complexes via a sol–gel process

Jianjun Ding^{a,b}, Bin Li^{a,*}, Haoran Zhang^{a,b}, Bingfu Lei^a, Wenlian Li^a

^a Key Laboratory of Excited State Processes, Changchun Institute of Optics Fine Mechanics and Physics, Chinese Academy of Sciences, Changchun 130033, PR China

^b Institute of Polyoxometalate Chemistry, Department of Chemistry, Northeast Normal University, Changchun 130024, PR China

Received 5 July 2006; accepted 13 November 2006

Available online 13 December 2006

Abstract

Organically modified silicate (ormosil) materials doped with [4,4'-dimethyl-2,2'-bipyridine-bis(2,2'-bipyridine)] ruthenium(II) dichloride ([Ru-mbpy]²⁺) and [4,4'-dimethylformate-2,2'-bipyridine-bis(2,2'-bipyridine)] ruthenium(II) dichloride ([Ru-dmfby]²⁺) were prepared by a sol–gel procedure for oxygen-sensing applications. The results indicated that the concentrations of the Ru(II) diimine complexes obviously influenced the linearity of Stern–Volmer plots (I_0/I vs. O₂%). The best suitable concentrations of [Ru-mbpy]²⁺ and [Ru-dmfby]²⁺ in the sol for oxygen sensors were found to be 1.0×10^{-3} M and 2.5×10^{-3} M, respectively. The fluorescence quenching time and recovery time of oxygen sensor doped with [Ru-mbpy]²⁺ (1.0×10^{-3} M) were 18 s and 38 s and those doped with [Ru-dmfby]²⁺ (1.0×10^{-3} M) were 13 s and 32 s, respectively. The oxygen sensor based on Ru(II) complex modified by esterification demonstrated excellent linear calibration relationship and improved long-term stability.

© 2006 Elsevier B.V. All rights reserved.

Keywords: Sol–gel; Ormosil; Ruthenium(II) complex; Oxygen sensor

1. Introduction

In comparison to the Clark-type amperometric electrodes, optical oxygen sensors possess many advantages such as zero oxygen consumption, no need for a reference electrode and immunity to exterior electromagnetic field interference [1,2]. Ru(II) diimine complexes have been widely used as photosensitizers because of their variety of attractive functions based on luminescence properties, such as strong visible absorption, efficient luminescence, high photochemical stability; especially a relatively long lifetime of metal-to-ligand charge transfer (MLCT) excited states. These unique features made them candidates for fluorescence quenching-based oxygen sensors [3,4].

Recently, the application of hybrid materials by bridging the organic and inorganic component at a molecular level has had

significant investigation [5,6]. The sol–gel approach has been used to develop new organic–inorganic hybrid materials [7–9]. The ormosil possessed the advantages both inorganic and organic characters such as easy realization of versatility in optical and mechanical properties. Therefore, the ormosil was often used as a matrix for the fabrication of optical oxygen sensors. The oxygen sensors based on immobilization of Ru(II) complexes in the ormosil hosts have been intensively investigated [7–17]. However, some performances parameters including the simplified calibration were still expected to further improved [3,8].

In an attempt to improve optical sensor properties, a method by modifying the molecular structure of Ru(II) complex has been adopted in this letter. The complex [Ru-mbpy]²⁺ and [Ru-dmfby]²⁺ were synthesized and selected as the photosensitizers, respectively. Oxygen sensors were prepared by sol–gel process, which hydrolyzed the mixture of tetraethoxysilane (TEOS) and *n*-octyltriethoxysilane (Octyl-triEOS) under the acid-catalyzing conditions. Octyl-triEOS was used as an organically modified precursor. The results showed that all

* Corresponding author. Fax: +86 431 6176935.

E-mail address: lib020@ciomp.ac.cn (B. Li).

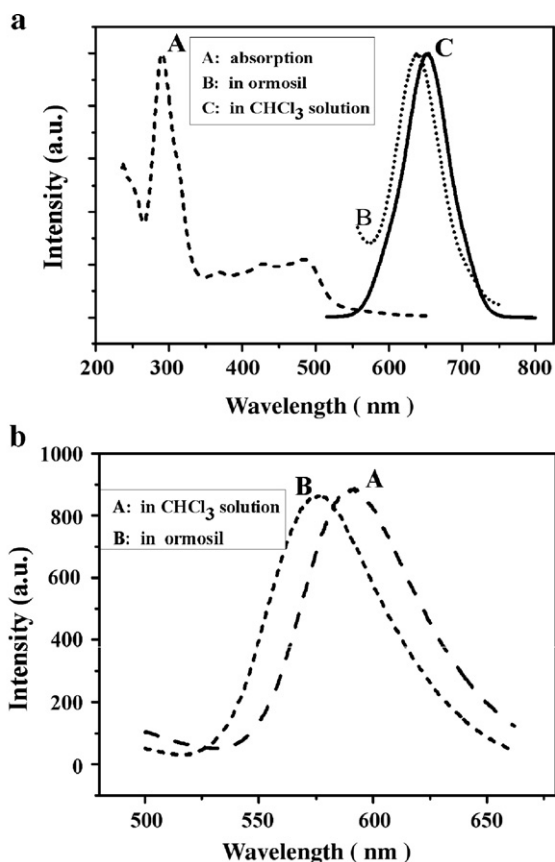


Fig. 1. (a) Absorption spectrum (A) and emission spectrum (C) of $[\text{Ru-dmfby}]^{2+}$ in CHCl_3 solution and emission spectrum of $[\text{Ru-dmfby}]^{2+}$ in ormosil (1.0×10^{-5} M) (B). (b) Emission spectra of $[\text{Ru-mbpy}]^{2+}$ in CHCl_3 solution (A) and $[\text{Ru-mbpy}]^{2+}$ in ormosil (1.0×10^{-5} M) (B).

oxygen sensors based on $[\text{Ru-mbpy}]^{2+}$ and $[\text{Ru-dmfby}]^{2+}$ exhibited long-term stability. Especially, the oxygen sensors based on $[\text{Ru-dmfby}]^{2+}$ modified by esterification showed higher sensitivity than that based on $[\text{Ru-mbpy}]^{2+}$. The relative luminescence intensity ratios in the absence to presence of oxygen were plotted against the oxygen concentration and so formed the Stern–Volmer plot. When the concentration of $[\text{Ru-dmfby}]^{2+}$ in the sol was 2.5×10^{-3} M, the Stern–Volmer plot was nearly linear.

2. Experimental

$[\text{Ru-mbpy}]^{2+}$ and $[\text{Ru-dmfby}]^{2+}$ were synthesized according to a literature procedure [18]. The sol–gel materials were prepared by modification of a reported method [19]: the precursor sols were prepared from a solution containing TEOS, Octyl-triEOS, HCl-acidified water, ethanol, and distilled water. The molar ratios of TEOS, Octyl-triEOS, ethanol and water were 1:1:4:4. TEOS and Octyl-triEOS were added into a clean plastic beaker. After the mixture were stirred for 30 min, HCl-acidified water (pH=2) was added to promote the hydrolysis and condensation of TEOS and Octyl-triEOS. The mixture was stirred continually at room temperature for 48 h. The Ru(II) complex was then added into the sol and the mixture was further stirred for 1 h. The concentration of Ru(II) complex was

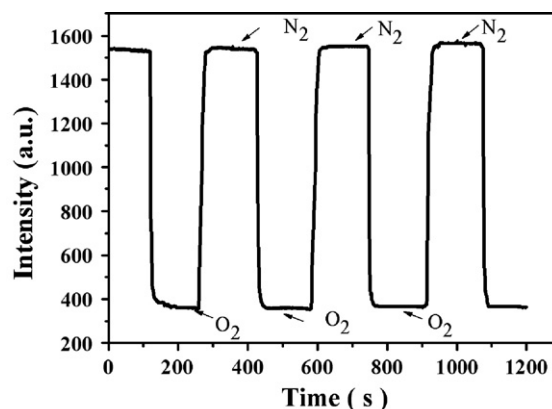


Fig. 2. Response time, relative intensity change and reproducibility of ormosil/ $[\text{Ru-dmfby}]^{2+}$ on switching between 100% nitrogen and 100% oxygen (Ru(II) complex concentration = 2.5×10^{-3} M).

expressed by its molar concentration in the sol. The resultant sol was divided into two sealed plastic cups and cured at 50°C in an oven for 2 weeks in order to complete the hydrolysis reaction and accomplish the gelation. Before any fluorescence measurement, in order to minimize photodecomposition of the gels, all samples were allowed to age in the dark for 6 and 12 months, respectively. All gels with different concentrations of $[\text{Ru-mbpy}]^{2+}$ or $[\text{Ru-dmfby}]^{2+}$ were prepared by the same procedure as abovementioned.

Fluorescence lifetime was obtained with a 266 nm light generated from the Fourth-Harmonic-Generator pump, which used the pulsed Nd:YAG laser as the excitation source. The Nd:YAG laser was with a line width of 1.0 cm^{-1} , pulse duration of 10 ns and repetition frequency of 10 Hz. A Rhodamine 6G dye pumped by the same Nd:YAG laser was used as the frequency-selective excitation source. The excitation and emission spectra were recorded with a Hitachi F-4500 fluorescence spectrophotometer equipped with a monochromator (resolution: 0.2 nm) and 150 W Xe lamp as the excitation source. Suitable filters were used to correct for the baseline shift due to any stray light. The oxygen sensor quenching data were measured by the Hitachi F-4500 fluorescence spectrophotometer. The oxygen and nitrogen were mixed together with different concentrations and passed via gas flow controllers directly to the sealed gas chamber for measurement. The solid diffuse-reflectance UV–VIS spectra were tested by PE UV–VIS Lambda 20.

3. Results and discussion

Fig. 1a shows the absorption and emission spectra of $[\text{Ru-dmfby}]^{2+}$ in CHCl_3 solution and emission spectrum of $[\text{Ru-dmfby}]^{2+}$ in ormosil,

Table 1
The response times (t_Q and t_R) of all oxygen sensors

Ormosil/ $[\text{Ru-mbpy}]^{2+}$	t_Q (ns)	t_R (ns)	Ormosil/ $[\text{Ru-dmfby}]^{2+}$	t_Q (ns)	t_R (ns)
1.0×10^{-3} M	18	38	1.0×10^{-3} M	13	32
2.5×10^{-3} M	24	45	2.5×10^{-3} M	15	40
5.0×10^{-3} M	35	58	5.0×10^{-3} M	23	47
7.5×10^{-3} M	42	70	7.5×10^{-3} M	32	58

Table 2
The sensitivities (I_0/I_{100}) of all oxygen sensors

Ormosil/[Ru-mbpy] ²⁺	6 m.	12 m.	Ormosil/[Ru-mbpy] ²⁺	6 m.	12 m.
1.0×10^{-3} M	2.86	2.74	1.0×10^{-3} M	2.75	2.68
2.5×10^{-3} M	2.63	2.58	2.5×10^{-3} M	4.11	3.95
5.0×10^{-3} M	2.33	2.28	5.0×10^{-3} M	3.06	2.96
7.5×10^{-3} M	2.03	1.98	7.5×10^{-3} M	2.38	2.24

6 m. and 12 m. are 6 and 12 months.

respectively. The fluorescence feature of [Ru-dmfbpy]²⁺ was the typical triplet MLCT process, which attributed to the transition from the ³MLCT excited state to the ground state of [Ru-dmfbpy]²⁺. The absorption spectrum of [Ru-dmfbpy]²⁺ showed strong peak at around 290 nm, which could be ascribed to ligand centered ($\pi \rightarrow \pi^*$) transitions and the broad absorption band centered at around 450 nm arises from the singlet MLCT state of [Ru-dmfbpy]²⁺ [19]. The emission peak of [Ru-dmfbpy]²⁺ in ormosil was located at 637 nm. The emission spectra of [Ru-mbpy]²⁺ in CHCl₃ solution and [Ru-mbpy]²⁺ in ormosil were shown in Fig. 1b. Both emission maximum wavelengths of the Ru(II) complexes in ormosil were found to be blue-shifted with respect to that in CHCl₃ solution (15 nm). This phenomenon could be explained as follows: in a rigid matrix, because the solvent could not reorient the Frank–Condon (unrelaxed) excited state was not completely stabilized or relaxed within its lifetime, and hence the emission occurred from a higher energy level than that in a fluid solution. This led to a blue shift in the emission of the Ru(II) complex when the surrounding media experience “fluid-to-glass” [19].

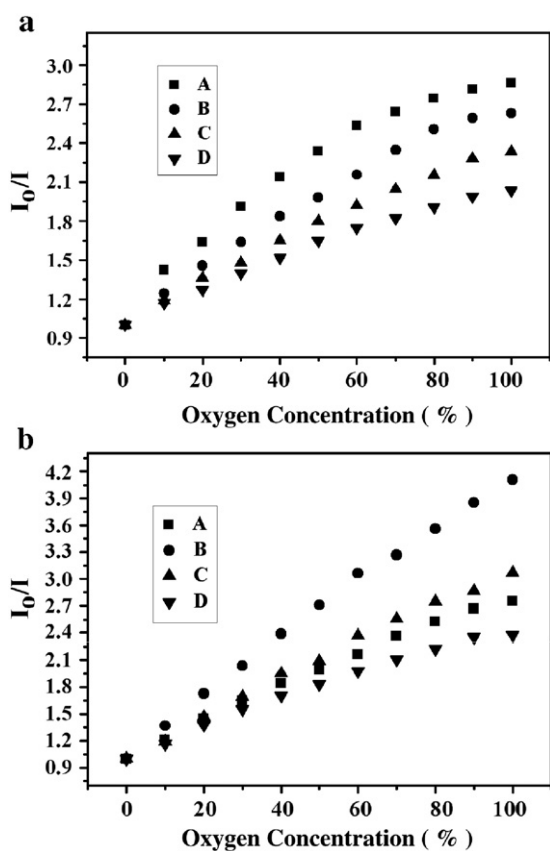


Fig. 3. Typical fluorescence intensity-based Stern–Volmer plots for: (a) ormosil/[Ru-mbpy]²⁺; (b) ormosil/[Ru-dmfbpy]²⁺ with different Ru(II) complex concentrations in the sol (A= 1.0×10^{-3} M, B= 2.5×10^{-3} M, C= 5.0×10^{-3} M, D= 7.5×10^{-3} M).

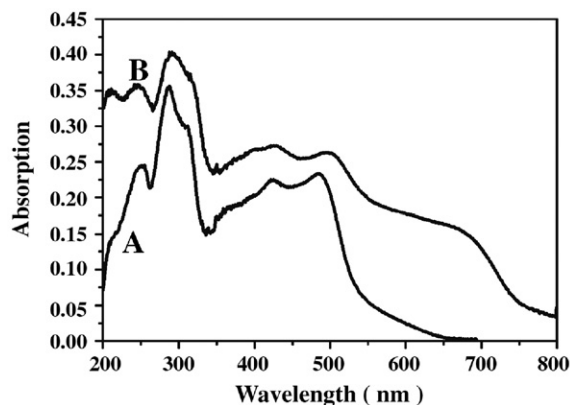


Fig. 4. The diffuse-reflectance spectra of ormosil/[Ru-dmfbpy]²⁺ (A) and [Ru-dmfbpy]²⁺ powder (B).

Oxygen fluorescence quenching studies were carried out by blowing nitrogen or oxygen over the samples. Equilibration was ensured until stable data were obtained. The calibrations of optical oxygen sensors are based on the following Stern–Volmer equation:

$$I_0/I = 1 + K_{SV}[O_2]$$

In this equation, I_0 and I were the luminescence intensities in the absence and presence of oxygen, respectively, and K_{SV} is the Stern–Volmer quenching constant.

The time required to achieve 95% of its full response was defined as quenching time (t_Q : ongoing from nitrogen to oxygen) and recovery time (t_R : ongoing from oxygen to nitrogen). Fig. 2 shows a typical dynamic response of ormosil/[Ru-dmfbpy]²⁺ on exposure to nitrogen and oxygen.

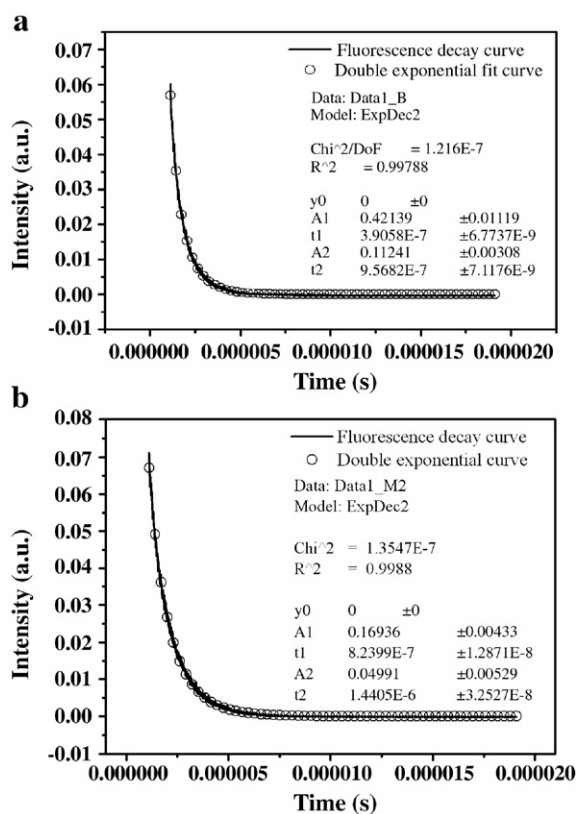


Fig. 5. Excited state decay curves of: (a) ormosil/[Ru-mbpy]²⁺, $\tau = 794.1$ ns; (b) ormosil/[Ru-dmfbpy]²⁺, $\tau = 1440.5$ ns.

The sensors based on ormosil/[Ru-dmfby]²⁺ demonstrated stable and reproducible signals, when Ru(II) complex concentration in the sol is 2.5×10^{-3} M. The response time of all oxygen sensors was listed in Table 1.

It was observed that t_Q and t_R increased with increasing concentration of Ru(II) complex. Furthermore, t_Q and t_R of ormosil/[Ru-dmfby]²⁺ were shorter than that of ormosil/[Ru-mbpy]²⁺, respectively.

Table 2 represented the sensitivities (I_0/I_{100} , I_{100} were the luminescence intensities in 100% oxygen) of all oxygen sensors, which were aged for 6 and 12 months, respectively. If error could be ignored, comparing the sensor aged for 12 months with that aged for 6 months, only a small change in I_0/I_{100} occurred. This suggested that all sensors showed long-term stabilities. It was attributed to the introduction of *n*-C₈H₁₇ group which acted as network modifiers and increased the overall ormosil hydrophobicity and flexibility. The xerogel shrinkage and pore collapse with time were overcome [11]. It was demonstrated that the Ru(II) complex was protected well by the ormosil matrices.

Fig. 3 shows the typical fluorescence intensity-based Stern–Volmer plots against oxygen concentrations. As seen in Fig. 3a, the oxygen sensors based on the ormosil/[Ru-mbpy]²⁺ showed non-linear Stern–Volmer plots. In addition, the values of I_0/I_{100} decreased with increasing the concentration of [Ru-mbpy]²⁺. In Fig. 3b, the nearly linear Stern–Volmer plot was obtained from the oxygen sensor based on [Ru-dmfby]²⁺ which was fabricated at the concentration of 7.5×10^{-3} M. When the concentration of [Ru-dmfby]²⁺ in the sol was increased from 1.0×10^{-3} to 7.5×10^{-3} M, the values of I_0/I_{100} increased first and then decreased. It was found that 2.5×10^{-3} M was the best concentration for ormosil/[Ru-dmfby]²⁺. The highest sensitivity and good linear plot were obtained at this condition. These results should be largely attributed to the reduced concentration quenching through introducing a sterically hindered spacer COOC₄H₉ in [Ru-dmfby]²⁺ molecule.

Fig. 4 shows the solid diffuse-reflectance UV–VIS spectra of [Ru-dmfby]²⁺ and ormosil/[Ru-dmfby]²⁺. Both sets of data could be fitted blue shifts of the low energy absorption bands, which was observed in spectra of the Ru(II) complex within ormosil relative to that in solid powder, and was attributed to rigidochromic effects [19]. The solid diffuse-reflectance UV–VIS spectrum of ormosil/[Ru-dmfby]²⁺ was very similar to that of [Ru-dmfby]²⁺, indicating that the molecule remained intact during the process of encapsulation.

Fig. 5a and b represented the typical excited state intensity decay curves of ormosil/[Ru-mbpy]²⁺ and ormosil/[Ru-dmfby]²⁺ in air, respectively. Both could be well fitted by the double exponential decay mode. It was found that the luminescence lifetime of [Ru-dmfby]²⁺ (1440.5 ns) became longer than that of [Ru-mbpy]²⁺ (794.1 ns) in ormosil, leading to improvement on oxygen sensor properties.

4. Conclusions

Ormosil/[Ru-dmfby]²⁺ has been demonstrated to be a suitable candidate for optical oxygen sensor compare to

ormosil/[Ru-mbpy]²⁺. A linear Stern–Volmer plot indicated that the oxygen sensors were stable under different oxygen concentrations. As expected, by introducing a sterically hindered spacer COOC₄H₉ in the Ru(II) molecule, the linearity improvement of Stern–Volmer plot was achieved. Furthermore, the fluorescence lifetime and the sensitivities were improved and the oxygen sensors exhibited long term stability over 12 months. The results suggest that molecular engineering is an effective method to enhance the performance of oxygen sensor based on organic metal complexes.

Acknowledgements

The authors gratefully thank the financial supports of One Hundred Talents Project from Chinese Academy of Sciences, and the National Natural Science Foundations of China (Grant No. 20571071).

References

- [1] M.M.F. Choi, D. Xiao, *Analyst* 124 (1999) 695.
- [2] W.Y. Xu, R.C. McDonough III, B. Langsdorf, J.N. Demas, B.A. DeGraff, *Anal. Chem.* 66 (1994) 4133.
- [3] M.T. Murtagh, M.R. Shahriari, *Chem. Mater.* 10 (1998) 3862.
- [4] P. Zhang, J.H. Guo, Y. Wang, W. Pang, *Mater. Lett.* 53 (2002) 400.
- [5] A. Walcarius, *Chem. Mater.* 13 (2001) 3351.
- [6] Y.H. Li, H.J. Zhang, H.R. Li, J. Lin, Y.Y. Yu, Q.G. Meng, *Mater. Lett.* 56 (2002) 597.
- [7] A.C. Franville, D. Zambon, R. Mahiou, *Chem. Mater.* 12 (2000) 428.
- [8] X. Chen, Z.M. Zhong, Z. Li, Y.Q. Jiang, X.R. Wang, K.Y. Wong, *Sens. Actuators, B, Chem.* 87 (2002) 233.
- [9] C. Malins, S. Fanni, H.G. Glever, Bran D. MacCraith, *Anal. Commun.* 36 (1999) 3.
- [10] N. Leventis, A.-M.M. Rawashdeh, I.A. Elder, J.H. Yang, A. Dass, C. Sotrious-Leventis, *Chem. Mater.* 16 (2004) 1493.
- [11] P.N. Deepa, M. Kanungo, G. Claycomb, P.M.A. Sherwood, M. Collinson, *Anal. Chem.* 75 (2003) 5399.
- [12] Y. Tang, E.C. Tehan, Z.Y. Tao, F.V. Bright, *Anal. Chem.* 75 (2003) 2407–2413.
- [13] Y. Amao, K. Asai, I. Okura, *Anal. Chim. Acta* 407 (2000) 41.
- [14] C.M. Chan, M.Y. Chan, M. Zhang, W. Lo, K.Y. Wong, *Analyst* 124 (1999) 691.
- [15] P. Douglas, K. Eaton, *Sens. Actuators, B, Chem.* 82 (2002) 48.
- [16] Y. Amao, I. Okura, *Sens. Actuators, B, Chem.* 88 (2003) 162.
- [17] H. Chuang, M.A. Arnold, *Anal. Chim. Acta* 368 (1998) 83.
- [18] G. Sprintschnik, H.W. Sprintschnik, P.P. Kirsch, *J. Am. Chem. Soc.* 99 (15) (1977) 4947.
- [19] P. Innocenzi, H. Kozuka, T. Yoko, *J. Phys. Chem., B* 101 (1997) 2285.